

Ligand-Induced Changes in Membrane-Bound Acetylcholine Receptor Observed by Ethidium Fluorescence. 2. Stopped-Flow Studies with Agonists and Antagonists[†]

Ulrich Quast,[‡] Michael I. Schimerlik,[§] and Michael A. Raftery*

ABSTRACT: The kinetics of cholinergic ligand binding to membrane-bound acetylcholine receptor from *Torpedo californica* have been followed in a stopped-flow photometer, by using the fluorescent probe ethidium. The overall reaction amplitude, as a function of ligand concentration, can be fit to the law of mass action for both agonists and antagonists. All agonists show at least biphasic kinetics, and the concentration dependence of the kinetic parameters is fit by a

common mechanism involving sequential binding of ligands with increasingly lower affinity. The receptor–ligand precomplexes isomerize to different noninterconvertible final complexes depending on the number of ligands bound. In contrast, the kinetics observed with antagonists cannot be fit to a common model. These kinetics are always much slower than those observed with agonists, and the relaxation rates depend only weakly on antagonist concentration.

Various signals have been used to observe the interaction of cholinergic ligands with AcChR¹ preparations in *in vitro* studies. The most direct method followed the changes in intrinsic fluorescence accompanying ligand binding (Bonner et al., 1976; Barrantes, 1976). The small overall change in fluorescence ($\leq 1\%$) superimposed on a large nonspecific fluorescence decrease renders these experiments extremely difficult. The inhibition of the rate of toxin binding to the receptor by cholinergic ligands provided an indirect signal by which slow ligand-induced changes in the affinity state of the AcChR were detected (Weber et al., 1975; Colquhoun & Rang, 1976; Weiland et al., 1976, 1977; Lee et al., 1977; Quast et al., 1978b). The interpretation of the data obtained in this way requires a careful study of the mechanism of toxin binding and the perturbation thereof by the ligand under study (see, e.g., Quast et al., 1978b). Recently, extrinsic fluorescent probes like quinacrine (Grünhagen & Changeux, 1976; Grünhagen et al., 1976, 1977) and ethidium (Schimerlik & Raftery, 1976; Quast et al., 1978a) have been used to monitor the kinetics of ligand binding to membrane-bound AcChR. Obviously, the interpretation of such data depends on a careful analysis of the interaction of the indicator dye with the membrane fragments.

In the preceding communication (Schimerlik et al., 1979a), it was shown that the fluorescence increase observed after mixing receptor–Eth complex with cholinergic ligands reflects specific ligand–receptor interactions since (1) no fluorescence increase is observed when receptor–toxin complex (which does not bind ligand in a specific manner; see, e.g., Weber & Changeux, 1974) was mixed with ligand and (2) the fluorescence increase observed after mixing receptor–ethidium complex with varying ligand concentrations is described by the law of mass action, yielding equilibrium constants consistent with those observed by other methods. For the ligand Carb it was shown that the fluorescence increase was due to

an increase in the quantum yield of bound Eth rather than to a dye uptake. Moreover, Eth does not seem to extensively alter the state of the membrane-bound receptor (see Schimerlik et al. (1979a)). In this paper we present the kinetics of the interaction of cholinergic agonists and antagonists with membrane-bound AcChR in the presence of Eth, as observed in a stopped-flow photometer, and we discuss fitting of the results to a variety of mechanisms.

Experimental Section

Torpedo californica membrane fragments, enriched in AcChR, were prepared as referenced in the preceding paper of this issue (Schimerlik et al., 1979a). The affinity state of membrane-bound AcChR was determined according to Quast et al. (1978b). The chemicals used are listed in the preceding paper.

Rapid mixing experiments were done in a Durrum stopped-flow photometer, Model D-110 (dead time ≈ 2.5 ms), set up in the fluorescence mode. The instrument was connected to a Tektronix 5103N storage oscilloscope and/or a Biomation Model 805 transient recorder and a Hewlett-Packard 7004 X-Y recorder. Excitation was at 493 ± 5 nm and emission was monitored by using a Corning C.S. 3–69 cutoff filter. Typical conditions were as follows. Membrane fragments (0.3 – $0.5 \mu\text{M}$ in $[^{125}\text{I}]\text{-}\alpha\text{-BuTx}$ sites) and Eth ($2 \mu\text{M}$) in one syringe were mixed with Eth ($2 \mu\text{M}$) and ligand in the other. All solutions were prepared in *Torpedo* Ringer's solution containing 0.02% sodium azide (at pH 7.4), and temperature was maintained at 25°C .

Kinetic traces were analyzed by graphical methods (see, e.g., Figure 1). The fitting procedure of the kinetic parameters to mechanism 1 is described in the Appendix.

Results

(1) *Observations with Agonists.* (1.1) *Carbamylcholine. Qualitative Observations.* Mixing of membrane-bound receptor with cholinergic ligands in the presence of Eth resulted in an increase in Eth fluorescence (Schimerlik & Raftery,

[†] From the Church Laboratory of Chemical Biology, Division of Chemistry and Chemical Engineering, California Institute of Technology, Pasadena, California 91125. Received July 11, 1978; revised manuscript received December 15, 1978. Supported by U.S. Public Health Service Grants NS-10294 and GM-16424, by a grant from the Muscular Dystrophy Association of America, by a Deutsche Forschungsgemeinschaft Postdoctoral Fellowship (to U.Q.), and by a National Institutes of Health Fellowship (to M.S.).

[‡] Present address: Biozentrum, CH-4056, Basel, Switzerland.

[§] Present address: Department of Biochemistry and Biophysics, Oregon State University, Corvallis, OR 97330.

¹ Abbreviations used: AcCh, acetylcholine; AcChR, acetylcholine receptor; AcChE, acetylcholinesterase; $\alpha\text{-BuTx}$, $\alpha\text{-bungarotoxin}$; Carb, carbamylcholine; DAP, 1,10-bis(3-aminopyridinio)decane diiodide; DFP, diisopropyl fluorophosphate; Deca, decamethonium; *d*-Tc, *d*-tubocurarine; Eth, ethidium; Hexa, hexamethonium; *Torpedo* Ringer's solution, 20 mM Hepes buffer containing 250 mM NaCl, 5 mM KCl, 4 mM CaCl_2 , and 2 mM MgCl_2 , pH 7.4; $[\]_0$ denotes total concentration.

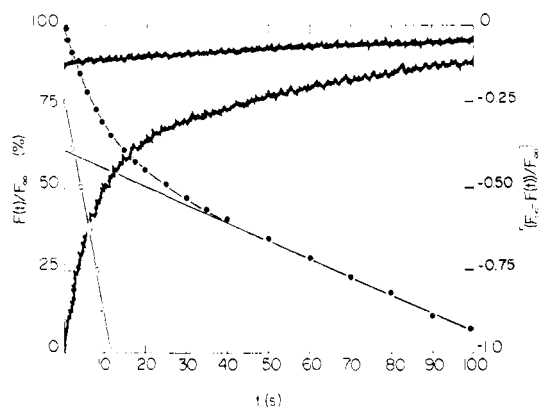


FIGURE 1: Kinetics of Carb interacting with AcChR in the low-affinity form in the presence of ethidium. One syringe of the stopped-flow photometer contained receptor (3×10^{-7} M in toxin sites) and Eth (2×10^{-6} M) and the other contained Carb (6×10^{-6} M) and Eth (2×10^{-6} M). The left ordinate shows the normalized increase in Eth fluorescence, $F(t)/F_{\infty}$ (the slow completion of the reaction is not shown). The right ordinate shows a semilogarithmic plot of the data (\bullet). Separation of the two phases gives for the slow (first) phase an amplitude $\delta A_1 = 43\%$ and a relaxation rate $\tau_1^{-1} = 1.2 \times 10^{-2} \text{ s}^{-1}$ and for the second (fast) phase (\circ) $\delta A_2 = 57\%$ and $\tau_2^{-1} = 0.15 \text{ s}^{-1}$.

1976; Schimerlik et al., 1979a). Use of the stopped-flow technique provided the time resolution for an accurate examination of the kinetics of that increase (Quast et al., 1978a). In order to ensure that the observed effect was specific, the following control experiments were undertaken: (a) rapid mixing of membrane fragments, originally in the low-affinity form, with buffer in the stopped-flow photometer, did not change the affinity state of the receptor as determined by the assay described by Quast et al. (1978b); (b) mixing of membrane fragments in the absence of Eth with buffer or ligands did not result in any detectable changes in light scattering; and (c) in the presence of Eth mixing of receptor with buffer or mixing of receptor-toxin complex with cholinergic ligands did not show any significant change in Eth fluorescence.

When Carb at concentrations less than $1 \mu\text{M}$ was mixed with receptor originally in the low-affinity form (Weber et al., 1975; Lee et al., 1977; Quast et al., 1978b), the fluorescence increase of bound Eth followed a single slow exponential with a half-time in the minute range (phase 1). At higher ligand concentrations, a faster phase arose (phase 2). Figure 1 shows a kinetic trace measured at a final Carb concentration of $3 \mu\text{M}$ where the amplitudes of both phases were about equal. With increasing ligand concentration, the amplitude δA_2 [see Figure 2 (\circ)] and the relaxation rate τ_2^{-1} [Figure 2 (Δ)] of phase 2 increased. Correspondingly, phase 1 decreased in both amplitude and relaxation rate [see Figure 2 (\blacktriangle)]. At Carb concentrations higher than $50 \mu\text{M}$ only the second phase remained with its amplitude, δA_2 , rapidly reaching a constant value. The observed rate, τ_2^{-1} , also began to level off although a plateau value was not yet reached at a Carb concentration of 1 mM . The total amplitude, δA_1 [Figure 2 (\bullet)], reached a plateau at Carb concentrations higher than $10 \mu\text{M}$.

The kinetic pattern described above was found consistently for Carb binding to the receptor with the exception that in many membrane preparations a third (very fast) exponential was observed at ligand concentrations higher than $500 \mu\text{M}$ (Quast et al., 1978a). Storage of membrane fragments for several days at 4°C , even in the absence of calcium (see also Grünhagen et al., 1976) generally resulted in faster kinetics for phase 2. In addition, a considerable slow decrease in fluorescence following the fast phase δA_2 was often observed

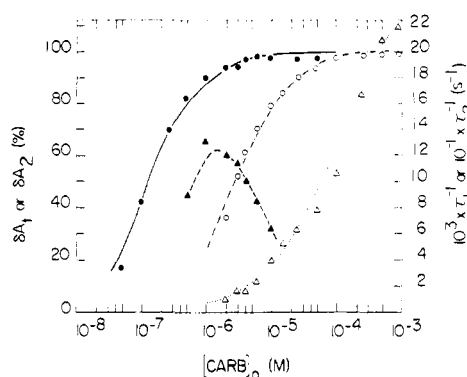
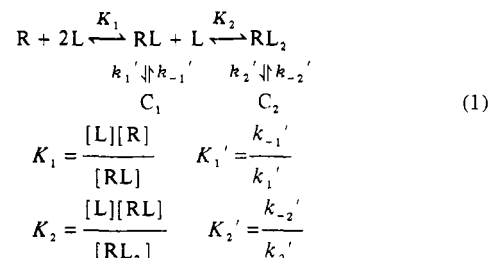


FIGURE 2: Kinetic parameters as a function of total Carb concentration. Left ordinate: total amplitude, δA_1 (\bullet), and amplitude of the fast phase, δA_2 (\circ), both in percent of δA_1 at saturation. Right ordinate: relaxation rates of the slow phase, τ_1^{-1} (\blacktriangle), and of the fast phase, τ_2^{-1} (Δ), respectively. The amplitude of the slow phase $\delta A_1 = \delta A_1 - \delta A_2$ is omitted for clarity. We calculated the curves using the parameters given in the first column of Table I according to eq A1 and A2 for δA_1 (—), eq 7 for δA_2 (---), eq 3 for τ_1^{-1} (---), and eq 2 for τ_2^{-1} (---). Conditions were identical with those for Figure 1.

at high Carb concentrations. Also, the saturation value of δA_1 was decreased. Similar aging phenomena were observed when a fresh receptor preparation was exposed to calcium and Eth at room temperature for more than 1 h. Often these effects made a quantitative evaluation of the slow kinetics at low ligand concentrations difficult.

Reaction Mechanism. Assuming that the fluorescence increase of Eth (a) directly reflects ligand-induced changes in the receptor and (b) that it is due to a change in quantum yield of bound Eth (see preceding paper), we found that the observed kinetics are consistent with the following mechanism where bound Eth is omitted.



First, the receptor R rapidly combines with ligand L, forming the two precomplexes RL and RL_2 . These precomplexes then isomerize slowly to the final complexes C_1 and C_2 with $\text{RL}_2 \rightarrow \text{C}_2$ faster than $\text{RL} \rightarrow \text{C}_1$. C_1 does not bind a further ligand molecule so that C_2 is exclusively formed from RL_2 . The increase in quantum yield comes from the isomerization steps $\text{RL}_i \rightarrow \text{C}_i$ ($i = 1$ and 2) and is assumed to be the same for both reactions (see below, eq 6).

The concentration dependence of the two kinetic phases expected from mechanism 1 is calculated in the Appendix. It can be rationalized as follows: at low ligand concentrations, $L/K_1 \gg L^2/(K_1 K_2)$, the law of mass action predicts that essentially no RL_2 will be formed. Consequently, only C_1 is formed, resulting in a single kinetic phase (slow phase or phase 1). At higher concentrations, both RL and RL_2 are formed in fast preequilibrium to the following isomerization steps. Since formation of C_2 is faster than that of C_1 , the pathway $\text{R} \rightarrow \text{RL} \rightarrow \text{RL}_2 \rightarrow \text{C}_2$ is first followed. This leads to a transient increase in concentration of C_2 above its equilibrium value $\bar{C}_2 = R_0 L^2 / (K_1 K_2 K_2')$ (fast phase = phase 2). Then the slower reaction $\text{RL} \rightarrow \text{C}_1$ occurs until the equilibrium distribution of \bar{C}_1/\bar{C}_2 is reached (slow phase = phase 1). With

Table I: Parameters for the Interaction of Agonists with AcChR in the Presence of 2 μ M Ethidium^a

ligand	K_1K_1' (μ M)	$K_1K_2K_2'$ (μ M ²)	K_{eff} (μ M)	k_2' (s ⁻¹)	k_{-2}' (s ⁻¹)	k_{-1}' (s ⁻¹)	k_1' (s ⁻¹)	K_1 (μ M)	K_2 (μ M)	δA_∞ (%) ^b	K_d (μ M) ^c
Carb ^d	0.10	2.60	30	2.3	0.10	2.0×10^{-3}	0.03	1.3	58.0	87 ± 5	0.12 ± 0.02 (0.07 ± 0.02)
Carb ^e	0.06	0.70	11	3.3	0.03	3.5×10^{-3}	0.06	1.3	8.5	?	0.057 ± 0.008 (0.07 ± 0.02)
Carb ^f	0.22	30.0	136	2.5	0.08	2.0×10^{-3}	0.03	3.8	320.0	?	(0.33 ± 0.05)
Deca	0.275	90.0	330	1.9	0.15	3.0×10^{-3}	0.12	10.0	200.0	100	0.18 ± 0.01
nicotine	0.40	20.0	40	1.4	0.14	2.0×10^{-3}	0.028	2.0	150.0	100	0.93 ± 0.11
choline ^g	20.0	>5000.0	>250	3.0	0.30	0.02	0.40	200	>500.0	92 ± 1	51.0 ± 3.6
thiocholine ^h	0.2	≈ 10	≈ 50	≥ 2.0	0.20	0.02	>0.05		>500.0	≈ 100	

^a For definition of symbols see eq 1 and 8. ^b $\delta A_\infty = \delta A_t$ at saturation with ligand expressed as percent of δA_t for Deca. ^c K_d determined from the inhibition of [¹²⁵I]- α -BuTx kinetics, except for the values in parentheses which were determined by ultracentrifugation with [³H]-Carb [Quast et al., 1978a; Schimerlik et al., 1979a (preceding paper)]. ^d Receptor originally in the low-affinity state (data shown in Figure 2). ^e AcChR originally in the high-affinity state (data shown in Quast et al. (1978a)), third phase at $L > 500 \mu$ M. ^f Titration in Ca²⁺ free *Torpedo* Ringer's solution; AcCh originally in the low-affinity form. ^g In vivo agonist (see, e.g., Adams (1975)). ^h In vivo agonist (Scott & Mauntner, 1964).

increasing ligand concentration, the law of mass action drives the equilibrium toward \bar{C}_2 , since $\bar{C}_1/\bar{C}_2 \approx (K_2K_2')/(K_1'L)$ (see eq A3). Therefore, the slow kinetic phase will disappear at high ligand concentrations.

As shown in the Appendix (see eq A8), the ligand-induced increase in fluorescence $F(t)$ contains two exponentials with the relaxation rates

$$\tau_2^{-1} \approx k_{-2}' + k_2' \frac{L^2/(K_1K_2)}{1 + L/K_1 + L^2/(K_1K_2)} \quad (2)$$

(see A6) for the fast phase and

$$\tau_1^{-1} \approx k_{-1}' + k_1' \frac{L/K_1}{1 + L/K_1 + L^2/(K_1K_2K_2')} \quad (3)$$

for the slow phase (see A7). The fast relaxation rate, τ_2^{-1} , describes formation of C_2 . It is decoupled from the slow reaction $RL \rightarrow C_1$ and reaches a limiting value of $k_{-2}' + k_1'$ at complete saturation of RL_2 . The slow relaxation rate, τ_1^{-1} , depends on the kinetic parameters of C_1 formation but also contains the equilibrium parameters for C_2 formation since the reaction $RL_2 \rightarrow C_2$ constitutes a fast preequilibrium to $RL \rightarrow C_1$. τ_1^{-1} first increases with increasing concentration of L , reflecting increasing saturation of RL , and then decreases as the reaction $RL_2 \rightarrow C_2$ is favored at high ligand concentrations (see Figure 2). τ_1^{-1} reaches a maximum value at the ligand concentration L_m where

$$L_m = \sqrt{K_1K_2K_2'} \quad (4)$$

This relation was used as a starting point for the determination of the overall equilibrium constant for formation of C_2 from R , $K_1K_2K_2'$. It is seen from Figure 2 (and for the other agonists studied; see, e.g., Figure 4) that the value of L_m is about 1 order of magnitude larger than the ligand concentration $L_{1/2}$ where δA_t is half-saturated. Therefore, δA_t , to a good approximation, reflects saturation of C_1 alone and one has

$$L_{1/2} \approx K_1K_1' + R_0/2 \quad (5)$$

Since δA_t remains constant in the concentration range where the contribution of \bar{C}_2 to the species present at equilibrium becomes increasingly significant [$L^2/(K_1K_2K_2') \gg 1$; see Figures 2 and 4], it follows that the increases in quantum yield, Q , accompanying the two isomerization reactions must be about equal. We have therefore set

$$Q_1 = Q_2 = Q \quad (6)$$

The amplitude of the fast phase, δA_2 , is given by (see A10)

$$\delta A_2 = Q[\bar{C}_1/(\tau_1k_{-2}') + \bar{C}_2/(\tau_1k_{-1}')] \quad (7)$$

The contribution of \bar{C}_1 to δA_2 is negligible, except at very low L since $\tau_1k_{-2}' \gg 1$ (see Figure 2 and Table I). The contribution of \bar{C}_2 is, however, heavily weighted by the factor $(\tau_1k_{-1}')^{-1}$ which varies with increasing ligand concentration from about 6 to 2 (see, e.g., Figure 2 and Table I) in the range where δA_2 and δA_1 are of the same order of magnitude. This reflects the overshoot phenomenon in C_2 (i.e., the transient concentration of C_2 is larger than the equilibrium concentration \bar{C}_2) due to the fact that $RL_2 \rightarrow C_2$ is in fast preequilibrium with $RL \rightarrow C_1$. The overshoot phenomenon, although correctly derived, has been neglected in our preliminary report on Carb kinetics (Quast et al., 1978a). This approximation led to a low value for the equilibrium constant for the additional ligand which is given by (8) (see eq A3).

$$K_{eff} = \frac{L\bar{C}_1}{\bar{C}_2} = \frac{K_2K_2'}{K_1'} \quad (8)$$

The parameters derived from a fit of the data shown in Figure 2 are listed in the first row of Table I. The sequence in which they are given reflects the extent to which they were directly obtained from the data (see Appendix). Table I also contains the parameters obtained for the reaction of Carb with receptor originally in the high-affinity form and with membrane fragments in the low-affinity state in the absence of calcium [for references on the affinity forms of AcChR see, e.g., Weber et al. (1975) and Quast et al. (1978b)]. The significance of the individual parameters as well as their variation with the experimental conditions will be treated in the Discussion.

In order to examine the reproducibility of the kinetics described above, a comparison was made of six kinetic titrations with different membrane preparations (conditions listed in Figure 1). In all cases, the values of the equilibrium constant for the first ligand, K_1K_1' were between 50 and 100 nM. The effective equilibrium constant for the second ligand, K_{eff} , varied within the limits $10 \mu\text{M} \leq K_{eff} \leq 30 \mu\text{M}$ and the rate constant k_2' varied within $2.3 \text{ s}^{-1} \leq k_2' \leq 5 \text{ s}^{-1}$. In three cases the "very fast" phase (phase 3) was detectable at concentrations higher than 300–500 μ M. The degree of variability of the kinetic parameters for the different membrane preparations mentioned above is comparable to that observed in other kinetic studies [see, e.g., Grünhagen et al. (1977)].

Ethidium Dependence. Figure 3 shows the Eth dependence of the Carb kinetics with the membrane preparation used in Figure 2, at a final Carb concentration of 2 μ M. The total amplitude, δA_t , decreased considerably at ethidium concentrations greater than 1 μ M [Figure 3 (●)], whereas the ratio $\delta A_2/\delta A_t$ increased (○). The relaxation rates depended only

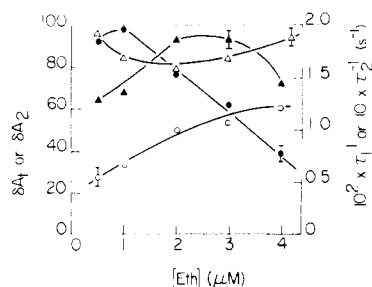


FIGURE 3: Ethidium dependence of the kinetic parameters. The final concentrations were $[\text{AcChR}]_0 = 1.5 \times 10^{-7} \text{ M}$ and $[\text{Carb}]_0 = 2 \times 10^{-6} \text{ M}$. The measurements were performed at a constant (low) photomultiplier voltage so that the total fluorescence (obtained after mixing of receptor plus ethidium with ethidium in the absence of Carb) increased linearly with ethidium concentration. The total amplitude (●) is given in arbitrary units; δA_2 (○) is normalized with respect to δA_1 (percent of δA_1 at the indicated $[\text{Eth}]_0$); $\delta A_1 = \delta A_t - \delta A_2$ is omitted. (▲) and (△) denote τ_1^{-1} and τ_2^{-1} , respectively. The error bars for each of the parameters denote the deviation from the mean value, determined from four individual experiments. The connecting curves have no theoretical significance.

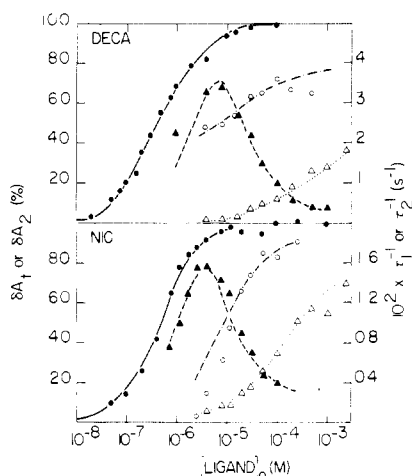


FIGURE 4: Kinetics of interaction of Deca and nicotine with the AcChR. The final concentrations were $[\text{AcChR}]_0 = 0.2 \mu\text{M}$ in $\alpha\text{-BuTx}$ sites, originally in the low-affinity form and $[\text{Eth}]_0 = 2 \mu\text{M}$. The symbols denote (●) δA_1 , normalized to 100% at saturation; (○) δA_2 (in percent of δA_1 at saturation); (▲) τ_1^{-1} ; and (△) τ_2^{-1} . The fitted curves were calculated as indicated in Figure 2 with the parameters from Table I.

weakly on Eth concentration. The Eth dependence of the kinetics was also measured at a final Carb concentration of $200 \mu\text{M}$ where only the fast phase remained (see Figure 2). The total amplitude $\delta A_t (= \delta A_2)$ showed the same concentration dependence as that seen in Figure 3 and τ_2^{-1} was independent of Eth concentration.

(1.2) *Deca, Nicotine, Choline, and Thiocholine.* All other agonists examined followed the kinetic pattern found for Carb except AcCh, which will be discussed in the next section. As examples, the data for Deca and nicotine are shown in Figure 4 together with the theoretical fits according to mechanism 1. The fitting parameters, together with those for choline and thiocholine, are listed in Table I. The very fast exponential at ligand concentrations higher than $500 \mu\text{M}$, which was occasionally observed with Carb and acetylcholine (see below), was also seen for thiocholine but not for any other agonist. As in the case of Carb, the equilibrium constants for the first ligand, $K_1 K_1'$, were much lower than the effective equilibrium constants for the second ligand, K_{eff} . The values of $K_1 K_1'$ were, in general, in agreement with the inhibition constants K_i for toxin binding kinetics (Table I) and vary over a broad concentration range, according to the ligand examined. The

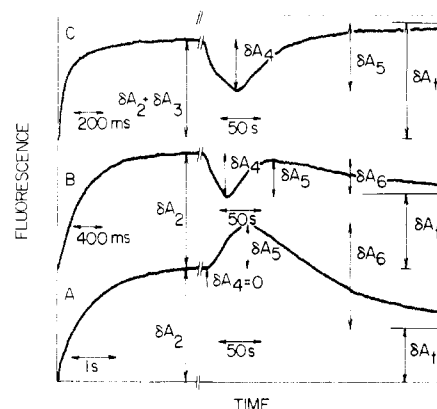


FIGURE 5: Kinetic traces after rapid mixing of AcChR with AcCh. Concentrations after mixing were $[\text{AcChR}]_0 = 0.5 \mu\text{M}$ in $\alpha\text{-BuTx}$ sites, originally in the low-affinity form; $[\text{Eth}]_0 = 1.5 \mu\text{M}$; and $[\text{AcCh}]_0 = 0.5 \text{ (A)}, 5 \text{ (B)}, \text{ and } 380 \mu\text{M (C)}$. Note the dual time base for the fast and the slow portion of the traces. Trace A is twofold expanded in vertical scale as compared to traces B and C. All amplitudes are given as percent of δA_t at saturation. Trace A ($[\text{AcCh}]_0 = 0.5 \mu\text{M}$): a fast increase in fluorescence ($\delta A_2 = 35\%$, $\tau_2^{-1} = 1 \text{ s}^{-1}$) is followed by a short lag phase ($\delta A_4 = 0$, $t_{1/2}(4) \approx 4 \text{ s}$, a fluorescence increase ($\delta A_5 = 16\%$, $t_{1/2}(5) = 11 \text{ s}$), and a final fluorescence decrease ($\delta A_6 = -30\%$, $t_{1/2}(6) = 100 \text{ s}$). Completion of the reaction is not shown but equilibrium level is indicated. The total amplitude is the difference between initial and final level of fluorescence, $\delta A_t = \sum \delta A_i = 18\%$ of δA_t at saturation. Trace B ($10 \mu\text{M}$): $\delta A_2 = 88\%$, $\tau_2^{-1} = 3 \text{ s}^{-1}$; $\delta A_4 = -30\%$, $t_{1/2}(4) = 10 \text{ s}$; $\delta A_5 = 24\%$, $t_{1/2}(5) = 15 \text{ s}$; $\delta A_6 = -27\%$, $t_{1/2}(6) = 100 \text{ s}$; $\delta A_t = 55\%$. Trace C ($380 \mu\text{M}$): $\delta A_2 = 33\%$, $\tau_2^{-1} = 3.5 \text{ s}^{-1}$; $\delta A_3 = 5\%$, $\tau_3^{-1} = 18 \text{ s}^{-1}$; $\delta A_4 = -42\%$, $t_{1/2}(4) = 8 \text{ s}$; $\delta A_5 = 53\%$, $t_{1/2}(5) = 40 \text{ s}$; $\delta A_6 = 0$; $\delta A_t = 95\%$.

kinetic parameters, however, did not vary strongly for the different ligands.

(1.3) *Acetylcholine.* The kinetics of acetylcholine differed from the basic agonist pattern on the slow time scale due to the action of AcChE (in our receptor preparation enzyme sites equaled about 1% of the concentration of toxin sites). Figure 5 shows kinetics traces of the Eth fluorescence increase obtained at different AcCh concentrations. On the fast time scale, there was, at lower concentrations, only the fast phase (phase 2, $\tau_2^{-1} \approx 1\text{--}3 \text{ s}^{-1}$). At high AcCh concentrations (Figure 5, trace C), an additional very fast phase appeared (phase 3, $\tau_3^{-1} \approx 18 \text{ s}^{-1}$). In the slow domain there was first an intermediate fluorescence decrease (phase 4, $t_{1/2}(4) \approx 5\text{--}10 \text{ s}$), followed by an increase (phase 5, $t_{1/2}(5) \approx 10 \text{ s}$) which then slowly relaxed to the equilibrium level (phase 6, $t_{1/2}(6) \approx 100 \text{ s}$). This last phase was missing at high ligand concentrations (see trace C). This kinetic pattern was reproducibly found with AcCh although the concentration at which the very fast phase appeared depended on the preparation as did the amplitude ratio between the intermediate fluorescence decrease and increase ($\delta A_4/\delta A_5$).

The complex reaction shown in Figure 5 reflects the fact that the receptor reacts with AcCh which is also hydrolyzed to choline by AcChE. It is therefore expected that the receptor finally relaxes to the state which would have been induced by initially mixing receptor with choline (equilibrium level). Indeed, the total fluorescence amplitude at equilibrium as a function of AcCh concentration is described by the law of mass action with an apparent K_d of $15 \mu\text{M}$ (data not shown). This value is close to that of choline (see Table I).

On the fast time scale, the second (fast) phase leveled off in both amplitude and rate at higher ligand concentrations as observed with all agonists (see Figures 2 and 4). At AcCh $> 50 \mu\text{M}$, $\delta A_2 \approx 90\%$ of δA_t and $\tau_2^{-1} \approx 4 \text{ s}^{-1}$. Above $50 \mu\text{M}$, a faster phase (phase 3, $\tau_3^{-1} \approx 17 \text{ s}^{-1}$) appeared at the expense of the second phase so that $\delta A_2 + \delta A_3 = \text{constant} = 90\% \delta A_t$.

Table II: Kinetics of AcChR with Antagonists

ligand	K_d (μM) ^a	K_i (μM) ^b	δA_∞ (%) ^c	kinetics	δA_2 (%) ^d	τ_1^{-1} (s ⁻¹) ^d	τ_2^{-1} (s ⁻¹) ^d
d-Tc	0.05	0.2 ± 0.02	76 ± 5	biphasic	≈20	0.02–0.04	≈0.05
Hexa	25.0	120 ± 14	87 ± 5	biphasic	≈20	≈0.020	≈0.55
DAP	1.90	4.7 ± 0.3	80 ± 10	monophasic	100	≈0.025	
gallamine	4.0	11 ± 1	44 ± 1	biphasic	concn dependent	≈0.01	0.04–0.02

^a Derived from concentration dependence of δA_t (see the legend of Figure 6). ^b Derived from inhibition of toxin binding kinetics (see preceding paper). ^c $\delta A_\infty = \delta A_t$ at saturation (in percent amplitude for Deca; see Table I). ^d δA_2 given in percent of δA_t at saturation for the ligand considered; subscripts 1 and 2 denote the slow and fast phase, respectively.

At still higher ligand concentrations, τ_2^{-1} started to decrease. The appearance of an additional fast phase at high ligand concentrations, also occasionally observed in the case of Carb (Quast et al., 1978a) and thiocholine (see above), will be dealt with in the Discussion.

The half-times of the slow phases (Figure 5, phases 4, 5, and 6) depended either weakly or not at all on AcCh concentration ($t_{1/2}(4) \approx 10$ s, $t_{1/2}(5) \approx 10$ –40 s, and $t_{1/2}(6) \approx 100$ s). In order to try to interpret the slow phases, the kinetics at $[\text{AcChR}]_0 = 10 \mu\text{M}$ were followed in the presence of increasing concentrations either of solubilized AcChE from *Electrophorus* or of the esterase inhibitors DFP and physostygmine or of a phospholipase fraction from *Bungarus caeruleus* (Bon & Changeux, 1975; Moody & Raftery, 1978). Total blockage of AcChE led to kinetics as observed with Carb: a fast increase in fluorescence (phase 2), followed by a small, much slower increase (phase 1). Incubation with lipase led, with increasing incubation time, to a threefold decrease in the overall amplitude and to the appearance of the very fast phase (phase 3) at the expense of phase 2 in the fast time domain. Incubation with solubilized AcChE from *Electrophorus* affected only the slow phases but left δA_t unchanged. At high concentrations of esterase, hydrolysis of $10 \mu\text{M}$ AcCh was complete in less than 1 s and yet the basic pattern of the AcCh kinetics was essentially conserved. This shows that a short contact of AcCh with the receptor was sufficient to condition the receptor for several minutes so that it reacted with choline in slow cycles of fluorescence decrease and increase (phases 4, 5, and 6). However, prolonged contact with AcCh (achieved by inhibition of the AcChE) resulted in the kinetic behavior found with the other agonists (see above).

(2) *Kinetics with Antagonists.* The kinetics observed after mixing receptor–Eth complex with various antagonists were very different from those measured with agonists. In general, the antagonist kinetics were biphasic with a poor separation in time of the two relaxation rates ($\tau_2^{-1} \approx 4\tau_1^{-1}$) (d-Tc; gallamine and Hexa; see Figure 6 and Table II). Only DAP gave monophasic kinetics. The total amplitude as a function of ligand concentration is well described by the law of mass action [see Figure 6 (●)]. In the cases of DAP and d-Tc, the total amplitude decreased at higher ligand concentrations due to displacement of the dye by the ligand (see preceding paper) especially in the case of DAP. This may lead to a considerable error in the calculated equilibrium constant, which was obtained from a weighted double-reciprocal plot of δA^{-1} vs. L^{-1} , by taking only the values at low ligand concentration into account. The concentration dependence of the two kinetic phases was in general weak, and the kinetics were slow. No common mechanism has been found to describe the kinetics. A survey of the empirically derived parameters is given in Table II.

Discussion

The fluorescence increase observed after mixing of receptor–Eth complex with a cholinergic ligand specifically reflects the interaction of that ligand with the membrane-

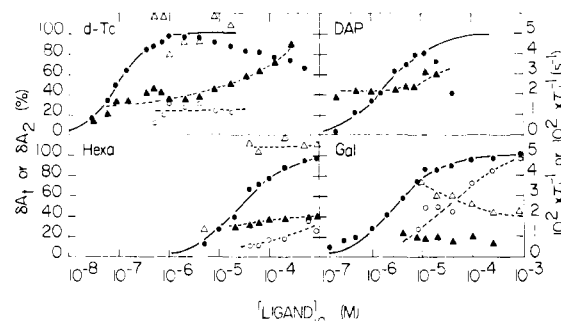


FIGURE 6: Concentration dependence of the kinetic parameters observed with various antagonists. Left upper panel: d-Tc. Left lower panel: Hexa. On the right side are DAP and flaxedil (gallamine). The symbols denote (●) total amplitudes, δA_t , normalized to a saturation value of 100%; (—) fit to δA_t according to the law of mass action, assuming a stoichiometry of 1:2 between ligand and toxin sites; (○) δA_2 (in percent of δA_t at saturation); (▲) and (△) τ_1^{-1} and τ_2^{-1} (s⁻¹). DAP showed only monophasic kinetics (see Table II for parameters). Typical concentrations after mixing were $[\text{AcChR}]_0 = 2 \times 10^{-7}$ M in α -BuTx sites (mostly in the low-affinity form) and $[\text{Eth}]_0 = 2 \mu\text{M}$.

bound AcChR, as shown in the preceding paper. Firstly, the receptor–toxin complex which does not bind ligands specifically (Weber & Changeux, 1974; Quast et al., 1978b) does not show any increase in ethidium fluorescence after addition of ligand. Secondly, the total fluorescence increase, as a function of added ligand concentration, is described by the law of mass action, and from this the equilibrium constant for that ligand can be calculated. The specificity of the Eth response is further confirmed by the kinetics of the ligand-induced fluorescence increase. As shown in this report, all agonist-induced kinetics consist of (at least) two phases. At low concentrations a slow phase was observed, and this was replaced at increasing ligand concentration by a fast phase with a time constant shorter than a second. In contrast, antagonist-induced kinetics did not follow a common pattern. In general, they show only a weak concentration dependence and were, in the ligand concentration range from 100 to 1000 μM , about 2 orders of magnitude slower than the kinetics with agonists. Note that this “pharmacological specificity” of the Eth response was also reflected in the kinetics measured with the agonist Deca and the antagonist Hexa [compare Grünhagen et al. (1977)].

The dependence of the kinetic parameters for Carb on Eth concentration (see Figure 3) is weak except for the total amplitude, δA_t . To a large degree this effect might reflect the nonlinear dependence of the quantum yield for Eth bound to the AcChR–Carb complex as was observed for Eth bound to the AcChR alone [see Schimerlik et al. (1979a) (preceding paper), Figure 2D]. On the other hand the decrease of δA_t with increasing Eth concentration might also reflect a weak perturbation of the membrane-bound receptor by the dye. This effect seems indicated by the weak dependence on Eth concentration of the rate of transition of AcChR from low to high affinity for Carb [see Schimerlik et al. (1979a) (preceding paper), Figure 8] or of the relaxation rate of HTX interacting with the AcChR [see Schimerlik et al. (1979b) (following

paper), Figure 2B]. Similarly, the increase of $\delta A_2/\delta A_1$ (see Figure 3) is interpreted as an Eth-induced shift of the equilibrium constant, for the second ligand, K_{eff} , toward lower values. A comparison of Carb titrations with Eth present at 1 or 2 μM shows that the K_{eff} varies by less than a factor of 2, so that the effect is small. The dependence of the observed relaxation rates on Eth concentration is weak and the limiting value of the fast rate, k_2' , does not depend on Eth. Overall, these effects are small and indicate that the state of the receptor is not radically changed by Eth concentration in the range 2–5 μM . This conclusion is confirmed by the observation that, at 2 μM , Eth does not interfere with agonist-induced ^{22}Na efflux from AcChR vesicles (H. P. Moore, P. Hortig, and M. Raftery, unpublished results).

The following discussion will be focused on some of the formal aspects of the mechanism established for agonists and on the interpretation of the fitting parameters. Finally, our results will be compared with those of a related study (Grünhagen et al., 1977).

Origin of the Kinetic Signal. The basic assumption leading to eq 1 is that the observed increase in fluorescence directly reflects conformational changes of the receptor–ligand complex for the ligand Carb. It was shown in the preceding communication that the increase in fluorescence intensity was caused by an increase in quantum yield of the membrane-bound Eth. This effect could be brought about by several mechanisms, e.g., (a) by a ligand-induced change of fluidity in the membrane which could produce a change in micro-environment of the bound Eth, (b) by a ligand-induced aggregation of the receptor in the membrane, (c) by direct interactions (e.g., electrostatic) arising upon the encounter of ligand with receptor–Eth complex, or (d) by a conformational change of the receptor–ligand complex affecting the environment of bound Eth. With respect to (a), a ligand-induced change in membrane fluidity seems unlikely in light of the measurements of fluorescence depolarization of pyrene bound to the membrane fragments in the presence and absence of cholinergic ligands (Martinez-Carrion et al., 1976). With respect to (b), we would expect that ligand-induced aggregation (e.g., dimerization) of the receptor would lead, in terms of the observed fluorescence increase, to strong Eth dependence of (at least one of) the relaxation rates and amplitudes. On the basis of the results in Figure 3 this possibility can be ruled out. With respect to (c), the concentration dependence of the observed relaxation rates and amplitudes is incompatible with the assumption that the kinetic signal reflects the encounter of ligand and receptor–ethidium complex. With respect to (d), the observation of slow and saturable relaxation rates is compatible with the assumption that the kinetic signal reflects ligand-induced conformational changes of the receptor–Eth complex. The change in kinetics with the pharmacological specificity (agonist or antagonist) of the ligand further supports this assumption. The observation by Witzemann & Raftery (1978b) of ligand-induced changes in the labeling pattern of the receptor subunits by the photoaffinity label Eth azide led to the conclusion that these ligands induce conformational changes in the membrane-bound receptor, involving several subunits. All these arguments strongly favor the hypothesis that the increase in quantum yield of the bound Eth reflects a ligand-induced conformational change of the receptor.

Reaction Mechanisms for Agonists. Having assigned the observed fluorescence changes to ligand-induced conformational changes in the receptor, we had to find a reaction mechanism which would allow for dramatic changes in agonist kinetics near saturation of the total amplitude: the first (slow)

phase decreased in both amplitude and relaxation rate as a faster phase arose with increasing ligand concentration. Some of the mechanisms examined are listed in Table III. First, mechanisms considering only two states of the receptor (R and R') and a single ligand molecule binding (Table III, 1–3) can be rejected on the basis of the calculated concentration dependence of the slow corresponding amplitude and relaxation rate. The fast relaxation rates which would reflect the ligand binding steps are not listed in Table III because they increase linearly with ligand concentration. (None of the experimental rates showed this property.) Mechanism 3 in Table III (the sum of (1) and (2)) is the two state model of receptor often used to describe desensitization of the receptor in vivo (Katz & Thesleff, 1957; Rang & Ritter, 1970) and in vitro [see, e.g., Weiland et al. (1977)]. Considering three state mechanisms of the receptor, a simple possibility is the sequential mechanism 4 in Table III, in terms of which Grünhagen et al. (1977) discussed their kinetics of agonist binding in the presence of the fluorescent local anaesthetic quinacrine. This mechanism predicts that both relaxation rates increase hyperbolically with ligand concentration (see Table III) and is therefore in disagreement with our observations. For the same reason, mechanisms involving a nonproductive binding state N were excluded, e.g., mechanism 5 in Table III.

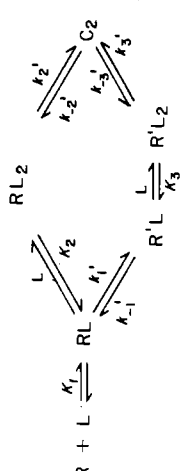
Turning to mechanisms involving two or more ligands binding to the receptor, we can first exclude the concerted transition model (MWC) since it predicts only a single slow relaxation time [for a review, see, e.g., Hammes & Wu (1974)]. Induced-fit models involving sequential binding of ligands allow for many permutations of ligand binding and isomerization steps [see, e.g., Loudon & Koshland (1972)]. The most simple example of these models, a linear sequence (Table III, 6), can be ruled out because of the concentration dependence of τ_1^{-1} . Note that high-affinity binding of the first ligand requires $k_1' \gg k_{-1}'$, so that τ_1^{-1} in (6) will ultimately increase with increasing L , in contrast to the experimental observations. As a more complex example of induced-fit models, it was considered that the same final complex was formed via two different kinetic pathways, depending on the number of ligands bound in the precomplexes, RL and RL₂ (see 7). This mechanism which is a simplified version of the model proposed by Bulger et al. (1977) for the interaction of [¹²⁵I]- α -BuTx with membrane-bound AcChR from *Electrophorus* predicts relaxation times in qualitative agreement with ours (see Figures 2 and 4). It requires, however, that the midpoints of δA_2 and τ_2^{-1} be close together and thus cannot be brought to a quantitative fit with the data. Eq 1 shows the only mechanism involving two ligands that we found compatible with the data.

It would have been desirable to obtain independent evidence for the low-affinity binding of a second ligand. However, binding studies with [³H]Carb are not feasible since, at AcChR concentrations high enough to detect the weaker dissociation constant (20–50 μM), specific binding of the ligand is obscured by a large nonspecific binding component.

Number of Ligands Bound. There is substantial evidence that the number of *high-affinity* ligand sites equals half the number of toxin sites in both membrane-bound [Raftery et al., 1975; Quast et al., 1978a; Schimerlik et al., 1979a (preceding communication)] and solubilized receptor (Moody et al., 1973; Maelicke et al., 1977). The number of toxin sites in the functional unit of the AcChR, is, however, still uncertain.

There is increasing evidence that the receptor occurs predominantly as a dimer in membrane preparations (Suarez-Isla & Hucho, 1977; Chang & Bock, 1977; Hamilton et

Table III: Kinetics of Mechanisms Considered for AcChR-Agonist Interaction

	mechanism	conditions ^a	(slow) kinetic relaxation	equilibrium amplitude δA_t
(1)	$R + L \xrightleftharpoons[k_{-1}]{k_1} RL \xrightleftharpoons[k_{-1}']{k_1'} R'L$	$z = R'L$	$\tau_1^{-1} = k_{-1}' + k_1' \frac{L}{L + K_1}; \delta A_1 \approx QR_0 \frac{L}{L + K_1 K_1'}$	$\delta A_t = \delta A_1$
(2)	$R \xrightleftharpoons[k_{-0}]{k_0} R' \xrightleftharpoons[k_{-1}]{L} R'L$	$z = R' + R'L; K_0' = \frac{R}{R'} \gg 1$	$\tau_1^{-1} = k_{-0}' + k_{-1}' \frac{\hat{K}_1}{L + \hat{K}_1}; \delta A_1 \approx QR_0 \frac{L}{L + \hat{K}_1/K_0'}$	$\delta A_t = \delta A_1$
(3)	$L + R \xrightleftharpoons[k_{-1}]{k_1} RL$ $k_0 \parallel k_{-0} \parallel k_1' \parallel k_{-1}'$ $L + R' \xrightleftharpoons[k_{-1}']{k_1'} R'L$	$z = R' + R'L; K_0' = \frac{R}{R'} \gg 1$	$\tau_1^{-1} = \frac{k_{-0}' + k_1' L/K_1}{1 + L/K_1} + \frac{k_{-0} + k_1 L/\hat{K}}{1 + L/\hat{K}}$ $\delta A_1 = QR_0 \frac{L}{L + \hat{K}_1/K_0'}$	$\delta A_t = \delta A_1$
(4)	$R + L \xrightleftharpoons[k_{-1}]{k_1} RL \xrightleftharpoons[k_{-1}']{k_1'} R'L \xrightleftharpoons[k_{-2}']{k_2'} R''L$	$z = Q_1 R'L + Q_2 R''L$ step 1' faster than 2''	$\tau_1^{-1} = k_{-1}'' + k_1'' \frac{L/(K_1 K_1')}{1 + L/K_1 K_1'}; \tau_2^{-1} = k_{-1}' + k_1' \frac{L/(K_1 K_1')}{1 + L/(K_1 K_1')}$ $\delta A_1 = QR_0 \frac{L}{L + \hat{K}_1/K_0'}$	$\delta A_t \approx Q_2 R_0 \frac{L/(K_1 K_1' K_1'')}{1 + L/(K_1 K_1' K_1'')}$
(5)	$N \xrightleftharpoons[k_{-1}]{k_1} R + L \xrightleftharpoons[k_{-2}]{k_2} RL \xrightleftharpoons[k_{-2}']{k_2'} R'L$	$z = N + R'L$ step 1 rate limiting	$\tau_1^{-1} \approx k_{-1} + k_1 \frac{L}{1 + L/(K_2 K_2')}; \tau_2^{-1} = k_{-2}' + k_2' \frac{L}{L + K_2}$	$\delta A_t \approx QR_0 \frac{L/K_1 + L/(K_2 K_2')}{1 + L/K_1 + L/(K_2 K_2')}$
(6)	$R \xrightleftharpoons[k_{-1}]{k_1} RL \xrightleftharpoons[k_{-1}']{k_1'} R'L \xrightleftharpoons[k_{-2}]{L} R'L_2 \xrightleftharpoons[k_{-2}']{k_2'} R''L_2$	$z = R'L + R'L_2 + R''L_2$ step 2' faster than 1' step 3' negligibly slow signal in 1', 2', and 3' $z = R'L + R'L_2 + C_2$	$\tau_1^{-1} = k_1' \frac{L}{L + K_1} + k_1' \frac{K_2 K_2'}{L + K_2 K_2'}; \tau_2^{-1} = k_{-2}' + k_2' \frac{L}{L + K_2}$ $\tau_1^{-1} = k_{-1}' + k_1' \frac{K_3}{K_3 + L} + k_1' \frac{L/K_1}{1 + L/K_1 + L^2/(K_1 K_2 K_2')}$ (+terms of 3'); $\delta A_1 \approx QR'L(1 - C_2/R_0)$	$\delta A_t \approx QR_0 \frac{L/(K_1 K_1') + L^2/(K_1 K_2 K_2')}{1 + L/(K_1 K_1') + L^2/(K_1 K_2 K_2')}$
				

^a Ligand L is buffered ($L_0 \gg R_0$), binding steps are considered fast as compared to the following isomerization reactions, and the corresponding relaxation rates are omitted. All isomerization rate constants are denoted with a prime. The isomerization equilibrium constants are defined as $K_i' = k_i'/k_i$ and are assumed to be much smaller than unity ($K_i' \ll 1$). z denotes the observed quantity; Q_i denotes different quantum yields. Kinetic phases are numbered starting with the slowest so that $\tau_1^{-1} \ll \tau_2^{-1}$. The bars denote equilibrium concentrations. The conditions for evaluation of the different mechanisms were chosen such that the predictions corresponded as closely as possible to the observed data.

al., 1977; Witzemann & Raftery, 1978a). To date it is not known which form, monomeric (two toxin sites) or dimeric (four toxin sites), is the basic functional form in the membrane or at the synapse, and therefore we have discussed our model in terms of the simplest receptor unit, i.e., the monomeric form which binds 2 mol of α -BuTx/mol of AcChR. This choice has the advantage of mathematical simplicity and the smaller number of fitting parameters required. The mechanism we propose for the monomeric receptor form (i.e., eq 1) cannot, however, accommodate the very fast phase (phase 3), observed occasionally at very high concentrations of the strongly binding ligands Carb, AcCh, and thiocholine. These results are fit instead by an expansion of eq 1 to the dimeric form of the receptor (see below). Phase 3 was not found with all membrane preparations and occurred more often with increasing age of the preparation. For these reasons we have not been able to collect sufficient reliable data for this phase. There is, however, substantial evidence that, at very high ligand concentrations, binding of a further ligand occurs and that, with an increasing shift of the membranes toward the high-affinity state, the equilibrium constant for the additional ligand decreases to experimentally attainable concentrations in the millimolar range. Formulation of a mechanism analogous to eq 1 for the dimeric receptor form includes binding of four ligands, two of them with high affinity. Binding of these two ligands leads first to the two precomplexes RL and RL_2 ; their respective isomerizations to C_1 and C_2 are reflected in the slow phase (phase 1). Formation of the triliganded complex C_3 from RL_2 would then be responsible for the fast phase (phase 2) and, the step $RL_2 \rightarrow C_4$ would be responsible for the very fast phase (phase 4).

A short mathematical analysis of this mechanism, considering only the first three ligands, has recently been published (Quast et al., 1978a). Since the four-ligand mechanism causes only an additional displacement of a complex of lower ligation (C_3) to C_4 on top of the earlier displacements, the mathematical treatment is placed in the Appendix.

Interpretation of Data. It has already been noted that the equilibrium constants for ligands obtained from the total amplitude are in good agreement with the value obtained by other methods, i.e., the inhibition of the rate of $[^{125}I]$ - α -BuTx binding (see Tables I and II) and ultracentrifugation experiments with $[^3H]$ Carb (see Table I). The overall reaction amplitude, δA_i , reflects essentially binding of the high-affinity ligand(s) (see text, eq 5), and the value of K_1K_1' correlates well with the inhibition constant K_i , found from the inhibition of the rate of α -BuTx binding to the AcChR. The four- to fivefold tighter binding of $[^3H]$ Carb in the presence of 4 mM Ca^{2+} obtained in ultracentrifugation studies (Table I, column 12) was also reflected in a change in K_1K_1' of two- to fourfold upon Ca^{2+} addition (Table I, column 2). This is in agreement with earlier work of Cohen et al. (1974) who found that Ca^{2+} increases the affinity of $[^3H]$ AcCh and Carb for AcChR by about twofold. The values of δA_i at saturation (see Tables I and II) were different when different ligands were tested on the same membrane preparation. Although the differences in δA_i were small for some ligands, they were statistically significant. These differences might be (partly) due to direct interactions between membrane-bound ligand and dye molecules; however, they may indicate either that the same final receptor conformation is induced by individual ligands to differing degrees [ligands as allosteric effectors; see, e.g., Janin, (1973)] or that each ligand induces a unique conformation. Although the differing kinetics observed for agonists and antagonists favor the latter interpretation, more detailed

spectroscopic studies are needed to decide between these possibilities.

Equation 1 with C_1 and C_2 both denoting the open channel form has recently been proposed as the mechanism describing channel opening at the frog neuromuscular junction (Stevens (1975) and personal communication). The thermodynamic parameters are, however, very different (especially $K_i' > 1$), and the time scale is in the millisecond range (Stevens, personal communication). Despite these differences the complete formal analogy is intriguing.

In low-affinity membrane preparations, the isomerization from low to high affinity for Carb, measured by an increase in the inhibition of the rate of $[^{125}I]$ - α -BuTx binding with incubation time, was observed in the presence of Eth [see Schimerlik et al. (1979a) (preceding paper)]. However, this did not seem to be reflected in the change in Eth fluorescence after mixing with Carb since the fast phase (phase 2) was about 10 times too fast and the slow phase had the wrong concentration dependence. A similar phenomenon has been observed by Briley & Changeux (1978) in a partially reconstituted membrane system where the slow agonist-induced affinity change was observed by the inhibition of α -toxin kinetics while only fast quinacrine responses were observed. A correlation between the slow ligand-induced change in affinity and the conformational changes reflected by Eth fluorescence is rather difficult since similar kinetics were found with Eth, regardless of whether the AcChR was "initially" in the low- or high-affinity form (see Table I). Since the assay for the affinity form of the AcChR (Quast et al., 1978b) is slow, it was impossible to decide whether receptor characterized as initially in the high affinity form was actually in that state prior to addition of ligand or underwent the isomerization to the high-affinity form at a much faster rate ($t_{1/2} < 5$ s) than receptor in the low-affinity form.

In a recent publication, Grünhagen et al. (1977) have analyzed the kinetics of agonist binding to receptor in the presence of the fluorescent local anaesthetic quinacrine. They observed a fast fluorescence increase in the millisecond time range, followed by a decrease in the minute range. Fitting the kinetics to mechanism 4 in Table III, they correlated the fast phase with channel activation and the slow phase with desensitization (see also Grünhagen & Changeux, 1976). This interpretation is, however, in question for the following reasons. (a) Electrophysiological experiments with various systems, using different methods, indicate that in vivo two agonist molecules are needed to open the ion channel, e.g., in *Electrophorus* electroplaque (Sheridan & Lester, 1977) or the frog neuromuscular junction [see, e.g., Dionne & Stevens (1975) and Adams (1975, 1977)]. In general, one would therefore expect a more complex ligand dependence of the rate constant corresponding to channel opening than that found by Grünhagen et al. (1977) (see also τ_2^{-1} in mechanism 4 of Table III). (b) Quinacrine at concentrations around 10 μ M acts as a noncompetitive inhibitor of the Carb-induced steady-state depolarization of the *Electrophorus* electroplaque (Grünhagen & Changeux, 1976). Therefore, one would expect a strong quinacrine dependence of the observed kinetics in vitro in the concentration range explored by Grünhagen et al. (1976, 1977), but none was found. Voltage-jump relaxation experiments on the frog end plate (Adams & Feltz, 1977) suggest that the fast phase of the kinetics in vitro (Grünhagen et al., 1977) might reflect channel blocking by the local anaesthetic quinacrine rather than activation of the channel. (c) No correlation was made between the observed kinetics and the original affinity state of the receptor for Carb. Despite these

differences concerning the interpretation of the kinetics with quinacrine, the specificity of the quinacrine response is established beyond doubt (Grünhagen & Changeux, 1976) as it is in the case of ethidium. The very fact, however, that two specific but indirect probes of receptor mechanism show such different kinetics upon addition of agonist suggests that correlation of these kinetics with electrophysiological results has to remain on a tentative basis.

Nevertheless, the kinetic studies presented here have provided useful information on the interactions of cholinergic ligands with membrane-bound AcChR. Firstly, the overall fluorescence amplitude of the reaction, δA_t , was an accurate measurement of the saturation of the receptor sites that bind ligands with high affinity. Secondly, the pharmacological specificity of agonists and antagonists was reflected in their different kinetic mechanisms. Finally and most important, the kinetic results require that more than a single ligand binds to the AcChR in vitro, in agreement with the stoichiometry deduced from electrophysiological studies in vivo.

Acknowledgments

The authors thank Dr. T. Moody for a generous gift of a phospholipase fraction prepared from *Bungarus caeruleus* venom. The technical assistance of J. Racs and the artwork and typing of Valerie Purvis are gratefully acknowledged.

Appendix

(1) *Two-Ligand Binding Mechanism* (eq 1 in text). (1.1) *Equilibrium*. By use of eq 6 in the text, $Q_1 = Q_2 = Q$, the total amplitude δA_t of the Eth fluorescence increase after addition of agonist is equal to

$$\delta A_t = Q(\bar{C}_1 + \bar{C}_2) \quad (A1)$$

where the bar denotes concentrations at equilibrium. Since K_1' and $K_2' \ll 1$ (see Table I), \bar{C}_1 and \bar{C}_2 can be approximated by

$$\bar{C}_1 \approx R_0 L / (K_1 K_1') \quad \bar{C}_2 \approx R_0 L^2 / (K_1 K_2 K_2') \quad (A2)$$

Here, R_0 is the total concentration of receptor units comprised of two toxin sites and L is the free ligand concentration. The ratio of \bar{C}_1 to \bar{C}_2 can be written as

$$\bar{C}_1 / \bar{C}_2 = (K_2 K_2') / (K_1' L) \equiv K_{\text{eff}} / L \quad (A3)$$

defining an effective equilibrium constant K_{eff} for the second ligand binding.

(1.2) *Kinetics*. The fluorescence signal F is proportional to $C_1 + C_2$ formed at time t

$$F = Q(C_1 + C_2). \quad (A4)$$

From mechanism 1 (see text) one obtains the rate equations²

$$\dot{C}_1 = k_1' RL - k_{-1}' C_1 \quad \dot{C}_2 = k_2' RL_2 - k_{-2}' C_2$$

Using the mass balance $R_0 = R + RL + RL_2 + C_1 + C_2$ and assuming that the binding steps in eq 1 of the text are fast [$RL = R \cdot L / K_1$; $RL_2 = R \cdot L^2 / (K_1 K_2)$], the differential equation can be rewritten, using matrix notation, as

$$\begin{pmatrix} \dot{C}_1 \\ \dot{C}_2 \end{pmatrix} + \mathbf{A} \begin{pmatrix} C_1 \\ C_2 \end{pmatrix} = \begin{pmatrix} q_1 \\ q_2 \end{pmatrix} R_0 \quad (A5)$$

where $q_1 = k_1' \phi L / K_1$, $q_2 = k_2' \phi L^2 / (K_1 K_2)$, $\phi = [1 + L / K_1 + L^2 / (K_1 K_2)]^{-1}$, and the elements of the reaction matrix \mathbf{A} are given by $a_{11} = q_1 + k_{-1}'$, $a_{12} = q_1$, $a_{21} = q_2$, and $a_{22} = q_2 + k_{-2}'$. The calculation of the relaxation rates is simplified by the fact that formation of C_2 is fast compared to formation

of C_1 . The fast relaxation rate, τ_2^{-1} ,

$$\tau_2^{-1} \approx k_{-2}' + k_2' \frac{L^2 / (K_1 K_2)}{1 + (L / K_1) + L^2 / (K_1 K_2)} \quad (A6)$$

is then obtained from the trace of \mathbf{A} , neglecting the terms containing k_1' and k_{-1}' . The slow relaxation rate, τ_1^{-1} , is calculated from $\tau_1^{-1} = \det \mathbf{A} / \tau_2^{-1}$ to equal

$$\tau_1^{-1} \approx k_{-1}' + k_1' \frac{L / K_1}{1 + (L / K_1) + L^2 / (K_1 K_2 K_2')} \quad (A7)$$

The fluorescence signal F is obtained by linear superposition of the solutions for C_1 and C_2

$$F = Q(C_1 + C_2) = \delta A_t - \delta A_1 e^{-t/\tau_1} - \delta A_2 e^{-t/\tau_2} \quad (A8)$$

with δA_t , τ_1^{-1} , and τ_2^{-1} from eq A1, A2, A6, and A7. The amplitudes δA_1 and δA_2 are calculated from the initial conditions

$$F(0) = 0 = \delta A_t - \delta A_1 - \delta A_2$$

$$\dot{F}(0) = QR_0 \phi [k_1' L / K_1 + k_2' L^2 / (K_1 K_2)] = \delta A_1 / \tau_1 + \delta A_2 / \tau_2$$

Neglecting small terms of the order of $\tau_1^{-1} / \tau_2^{-1}$, one obtains

$$\delta A_1 = +Q[\bar{C}_1[1 - (\tau_1 k_{-2}')^{-1}] + \bar{C}_2[1 - (\tau_1 k_{-1}')^{-1}]] \quad (A9)$$

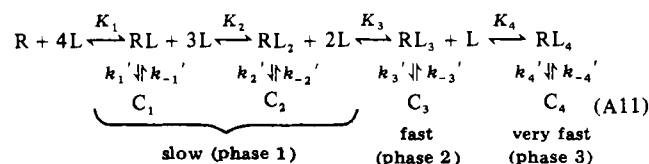
$$\delta A_2 = +Q[\bar{C}_1 / (\tau_1 k_{-2}') + \bar{C}_2 / (\tau_1 k_{-1}')] \quad (A10)$$

(1.3) *Fitting Procedure*. The total amplitude, δA_t , was calculated according to eq A1 and A2 for a given concentration of the free ligand, L . The total ligand concentration, L_0 , was then calculated from $L_0 = L + \bar{C}_1 + 2\bar{C}_2$ and a plot of δA_t vs. L_0 was constructed. For the start of the fitting procedure, $K_1 K_1'$ was taken from the midpoint of the plot δA vs. L ($L_{1/2} \approx K_1 K_1' + R_0 / 2$) and the value of $K_1 K_2 K_2'$ from the concentration where τ_1^{-1} reaches its maximum value or starts to decline (see text, eq 4 and 5). In general, only small variations of the starting guesses were necessary to obtain a satisfactory fit for δA_t vs. L_0 .

We calculated a second observable δA_2 according to eq A12 with the values of $K_1 K_1'$ and $K_1 K_2 K_2'$ determined from the fit for δA_t and using the experimental values of τ_1^{-1} , k_{-1}' and k_{-2}' . The calculation of δA_2 was very sensitive to small variations of τ_1^{-1} and k_{-1}' and these values were (slightly) varied until a good fit was achieved. δA_1 was calculated from $\delta A_1 = \delta A_t - \delta A_2$.

Next, τ_2^{-1} was fitted by using the experimental values of k_{-2}' and k_2' . [If k_2' could not be obtained directly from the experimental data (see, e.g., Figure 2), it was varied with the constraint $k_2' > 10k_{-2}'$.] $K_1 K_2$ was calculated from $K_1 K_2 K_2'$ (see δA_t) and K_2' . K_1 was varied until a good fit was obtained. In the last step τ_1^{-1} was calculated with k_1' as the only adjustable parameter with the constraint $k_1' \geq 10k_{-1}'$. In general, the five observed quantities δA_t , δA_1 , δA_2 , τ_1^{-1} , and τ_2^{-1} were well fit using a single consistent set of parameters (see Table I).

(2) *Four-Ligand Binding Mechanism*. In formal analogy to eq 1 (in text) this mechanism is written



where it is again assumed that (a) all isomerization steps $RL_i \rightleftharpoons C_i$ are accompanied by the same change in quantum yield,

² Dot denotes derivative with respect to time.

(b) all binding steps are fast, and (c) $K'_i = k_{-i}'/k_i' \ll 1$. At equilibrium we have

$$\bar{C}_i = RL_i/K'_i \text{ with } RL_i = RL^i / \prod_{j=1}^i K_j \quad i = 1, \dots, 4 \quad (\text{A12})$$

where all K_j are phenomenological (macroscopic) equilibrium constants, containing statistical weight factors. As discussed in a previous paper (Quast et al., 1978a), the parameters must be adjusted so that (a) a Scatchard plot regarding the two high-affinity sites (C_1 and C_2) is linear and (b) formation of $C_1 + C_2$ is reflected in one single kinetic phase. The condition for linearity of the Scatchard plot is that the equilibrium concentration of ligand bound to the two high-affinity sites, $L_B = \bar{C}_1 + 2\bar{C}_2$, reduces to a rectangular hyperbola as a function of L . Using eq A12 one obtains the equation

$$(2K_1K'_1)^2 = K_1K_2K'_2 \quad (\text{A13})$$

which differs from the corresponding equation given earlier (Quast et al., 1978a) by a statistical factor of 2, due to differing definitions of K_1 .

The rate equations for the final complexes are given by

$$C_i = k_i'RL_i - k_{-i}'C_i \quad i = 1, \dots, 4 \quad (\text{A14})$$

For the sum $X = C_1 + C_2$ one obtains

$$X = [k_1'L/K_1 + k_2'L^2/(K_1K_2)]R - k_{-1}'C_1 - k_{-2}'C_2 \quad (\text{A15})$$

The concentration of free receptor sites can be expressed as

$$R = (R_0 - X - C_3 - C_4)\phi \text{ with } \phi = [1 + \sum_{i=1}^4 L^i / \prod_{j=1}^i K_j]^{-1} \quad (\text{A16})$$

After insertion of eq A16 into eq A15 it becomes apparent that formation of X will be described by a single kinetic phase only if one assumes

$$k_{-1}' = k_{-2}' = k_{-3}' \quad (\text{A17})$$

The rate equations for X , C_3 , and C_4 can now be calculated in a straightforward manner. In the matrix form, they read

$$\begin{pmatrix} \dot{X} \\ \dot{C}_3 \\ \dot{C}_4 \end{pmatrix} + \begin{pmatrix} \beta\phi + k_{-3}' & \beta\phi & \beta\phi \\ \gamma\phi & \gamma\phi + k_{-3}' & \gamma\phi \\ \delta\phi & \delta\phi & \delta\phi + k_{-4}' \end{pmatrix} \begin{pmatrix} X \\ C_3 \\ C_4 \end{pmatrix} = \begin{pmatrix} \beta \\ \gamma \\ \delta \end{pmatrix} \phi R_0 \quad (\text{A18})$$

where

$$\begin{aligned} \beta &= k_1'L/K + k_2'L^2/(K_1K_2) \\ \gamma &= k_3'L^3 / \prod_{j=1}^3 K_j \\ \delta &= k_4'L^4 / \prod_{j=1}^4 K_j \end{aligned} \quad (\text{A19})$$

The relaxation rates, τ_i^{-1} , of the reaction matrix are calculated by successive approximations, with $\tau_1^{-1} \ll \tau_2^{-1} \ll \tau_3^{-1}$. They are

$$\begin{aligned} \tau_3^{-1} &\simeq \delta\phi + k_{-4}' \\ \tau_2^{-1} &\simeq \gamma[\phi^{-1} + \delta/k_{-4}']^{-1} + k_{-3}' \\ \tau_1^{-1} &\simeq \beta[\phi^{-1} + \delta/k_{-4}' + \gamma/k_{-3}']^{-1} + k_{-3}' \end{aligned} \quad (\text{A20})$$

and have the concentration dependence expected from mechanism A11 (see Discussion).

Calculation of the amplitudes pertaining to eq A18 from the initial conditions is tedious and leads to a complex mathematical expression. Since, however, at no concentration do more than two phases coexist, it is sufficient to consider eq A18 in the two concentration ranges where either (a) binding of the fourth ligand does not yet occur so that the

fluorescence signal is given by $F_a(t) = Q(X + C_3)$ or (b) the fourth ligand needs to be considered but X can be neglected so that $F_b(t) = Q(C_3 + C_4)$. Then the formalism developed in eq A8–A10 holds, and one can write by direct analogy

$$F_a(t) = Q(X + C_3) = \delta A_1 - \delta A_1 e^{-t/\tau_1} - \delta A_2 e^{-t/\tau_2} \quad (\text{A21})$$

with $\delta A_1 = \bar{X} + \bar{C}_3$, $\delta A_2 \simeq Q\bar{X}/(\tau_1 k_{-3}') + Q\bar{C}_3/(\tau_1 k_{-3}')$, and $\delta A_1 = \delta A_1 - \delta A_2$ (see eq A12, A20). Correspondingly in the high concentration range

$$F_b(t) = Q(C_3 + C_4) = QR_0 - \delta A_2 e^{-t/\tau_2} - \delta A_3 e^{-t/\tau_3} \quad (\text{A22})$$

with $\delta A_3 \simeq Q\bar{C}_3/(\tau_2 k_{-4}') + Q\bar{C}_4/(\tau_2 k_{-4}')$ and $\delta A_2 = QR_0 - \delta A_3$.

References

- Adams, P. R. (1975) *Pfluegers Arch.* 360, 145–153.
- Adams, P. R. (1977) *J. Physiol. (London)* 268, 271–289.
- Adams, P. R., & Feltz, A. (1977) *Nature (London)* 269, 609–611.
- Barrantes, F. J. (1976) *Biochem. Biophys. Res. Commun.* 72, 479–488.
- Bon, C., & Changeux, J.-P. (1975) *FEBS Lett.* 59, 212–216.
- Bonner, R., Barantes, F. J., & Jovin, T. M. (1976) *Nature (London)* 263, 429–431.
- Briley, M. A., & Changeux, J.-P. (1978) *Eur. J. Biochem.* 84, 429–439.
- Cohen, J. B., Weber, M., & Changeux, J.-P. (1974) *Mol. Pharmacol.* 10, 904–932.
- Colquhoun, D., & Rang, H. P. (1976) *Mol. Pharmacol.* 12, 519–539.
- Dionne, V. E., & Stevens, C. F. (1975) *J. Physiol. (London)* 251, 245–270.
- Grünhagen, H. H., & Changeux, J.-P. (1976) *J. Mol. Biol.* 106, 479–516, 517–535.
- Grünhagen, H. H., Iwatsubo, M., & Changeux, J.-P. (1976) *C. R. Hebd. Seances Acad. Sci., Ser. D* 283, 1105–1108.
- Grünhagen, H. H., Iwatsubo, M., & Changeux, J.-P. (1977) *Eur. J. Biochem.* 80, 225–242.
- Hamilton, S. L., McLaughlin, M., & Karlin, A. (1977) *Biochem. Biophys. Res. Commun.* 79, 692–699.
- Hammes, G. G., & Wu, C.-W. (1974) *Annu. Rev. Biophys. Bioeng.* 3, 1–33.
- Janin, J. (1973) *Prog. Biophys. Mol. Biol.* 27, 77–120.
- Katz, B., & Thesleff, S. (1957) *J. Physiol. (London)* 138, 63–80.
- Lee, T., Witzemann, V., Schimerlik, M., & Raftery, M. A. (1977) *Arch. Biochem. Biophys.* 183, 57–63.
- Loudon, G. M., & Koshland, D. E. (1972) *Biochemistry* 11, 229–240.
- Martinez-Carrion, M., Raftery, M. A., Thomas, J. K., & Sator, V. (1976) *J. Supramol. Struct.* 4, 373–380.
- Moody, T., & Raftery, M. A. (1978) *Arch. Biophys. Biochem.* 189, 115.
- Quast, U., Schimerlik, M. I., & Raftery, M. A. (1978a) *Biochem. Biophys. Res. Commun.* 81, 864–955.
- Quast, U., Schimerlik, M. I., Lee, T., Witzemann, V., Blanchard, S., & Raftery, M. A. (1978b) *Biochemistry* 17, 2405–2414.
- Rang, H. P., & Ritter, J. M. (1970) *Mol. Pharmacol.* 6, 357–382.
- Schimerlik, M. I., Quast, U., & Raftery, M. A. (1979a) *Biochemistry* (sixth of 10 papers in this series).
- Schimerlik, M. I., Quast, U., & Raftery, M. A. (1979b)

- Biochemistry* (eighth of 10 papers in this series).
- Scott, K. A., & Mauntner, H. G. (1964) *Biochem. Pharmacol.* 13, 907.
- Sheridan, R., & Lester, H. A. (1977) *J. Gen. Physiol.* 70, 187-219.
- Stevens, C. F. (1975) *Cold Spring Harbor Symp. Quant. Biol.* XL, 169-173.
- Suarez-Isla, B. A., & Hucho, F. (1977) *FEBS Lett.* 75, 65-69.
- Weber, M., & Changeux, J.-P. (1974) *Mol. Pharmacol.* 10, 15-34.
- Weber, M., David-Pfeuty, T., & Changeux, J.-P. (1975) *Proc. Natl. Acad. Sci. U.S.A.* 72, 3443-3447.
- Weiland, G., Georgia, B., Wee, V. T., Chignell, C. F., & Taylor, P. (1976) *Mol. Pharmacol.* 12, 1091-1105.
- Weiland, G., Georgia, B., Chignell, C. F., & Taylor, P. (1977) *J. Biol. Chem.* 252, 7648-7656.
- Witzemann, V., & Raftery, M. A. (1978a) *Biochem. Biophys. Res. Commun.* 81, 1025-1031.
- Witzemann, V., & Raftery, M. A. (1978b) *Biochemistry* 17, 3598-3604.